THE INFLUENCE OF AIR CO-FLOW CHARACTERISTICS ON THE OSCILLATION OF A LIQUID SHEET

C. Siegler*, **A. Lozano***, **F. Barreras***
christian@litec.csic.es
***LITEC/CSIC, María de Luna 10, 50018 Zaragoza, Spain**

Introduction

Since the middle of the XX Century, break up of large-aspect ratio liquid sheets has been extensively studied (see, for example, [1], and references therein), especially in air-assisted or air-blasted configurations. Although most characteristics of the atomization processes in this specific geometry have been satisfactorily explained and the theories utilized to this end are by now well established and generally accepted, there are some other aspects that are still subject to controversy, and their justifications are still mere hypothesis.

Some of the more complex facets in the sheet break up are related to the air/liquid interaction and the interfacial phenomena. When studying these problems a major emphasis has been placed in analyzing the liquid behavior, looking at the influence of varying parameters such as velocity or thickness [2]. To understand the effect of the co-flowing gas, most studies have been limited to variations in the exit velocity [3], to determine the effect on the liquid sheet oscillations. It has been observed that the oscillation frequency depends linearly on the air velocity.

A point that has often been debated and has not been verified is the influence of the air channel width. This issue is related to the relevance, when describing the problem, of parameters such as to momentum flux ratio (MFR) or the total momentum ratio (MR) [4] and the role played by the air boundary layer thickness. The uncertainty is aggravated by the fact that up to date most conclusions have been drawn comparing results from different experiments in different conditions. This paper focuses in these aspects, and results, although still preliminary, are presented.

Experimental Installation - Atomizer Head and Geometric Conditions

Core of the experimental setup of the present study is the atomizer head with a contoured central slit nozzle for the liquid sheet, assisted by a pair of contoured channels for the co-flowing air. The central channel is made of two pieces of stainless steel; the air channels in the atomizer head are profiled by two aluminum pieces. Either of the channel pieces is fixed to a couple of brass plates. In this study experiments have been conducted for sheet thicknesses of d_l = 0.5 mm and and d_l=0.9 mm. The span of the nozzle was 80 mm. Experiments have been performed with three different air channel exit widths, d_l=$3.45; 9; 35$ mm corresponding to contraction ratios of 15.0, 5.2 and 1.5 respectively, as shown in table 1.

Channel	Width in mm	Contraction Ratio	Aspect Ratio
Water	0.5	16.1	160
	0.9	8.9	88.9
Air	3.45	15	22.6
	10	5.2	7.8
	35	1.5	2.2

Table 1: Contraction and aspect ratios of the two channels used for the present experiment

The water flow was fed through a couple of inlet pipelines with a controlled and regulated volumetric flow rate varying in a range from 60 to 640 l/h. The air flow was generated by a 5.5 kW fan (Casals, model AA 70 T2 7,5) whose speed was regulated with a Danfoss frequency regulator. A calibration was performed for each geometry to relate fan frequency with air exit velocity.

Measurement Equipment

A standard laser diffraction technique has been used to measure the sheet oscillation frequencies. As in detail described in [3], the beam of a single 5 mW laser diode was directed to a photodiode, which registered the oscillating behaviour of the liquid sheet by the incoming laser signal. A maximum of the signal was registered when the beam was not disturbed nor blocked by the water sheet, whereas a minimum was noted for the moments when the sheet passed the beam cutting and dispersing the laser light. The registered signal was monitored by a digital Oscilloscope (model Tektronix TDS3012), with an FFT module (TDS3FFT) to calculate the power spectrum.

Results and Discussion

To ease the comparison of the results, the same plots will be presented for all the geometries under study. Water exit velocities were varied from u_l = 0.38 m/s to 4.94 m/s. For each value of the water volumetric flowrate, seven air stream velocities were applied, u_g= $20; 25; 35; 45; 55; 65; 75$ m/s, except for the air channel of d_g= 35 mm, where u_g= 75 m/s could not be achieved. The first plot depicts the sheet oscillation frequency f_{osc} as a function of the water velocity u_l for the different air velocities u_g. Following Mansour and Chigier [3], the curves in these charts can be divided into three characteristic zones (A,B,C) in dependence on the oscillation behavior of the sheet. In zone A the high air/water velocity ratio causes to sheet to separate in filaments immediately after exiting the nozzle, and in some cases a single oscillation frequency is not clearly defined. In zone B, a dominant sinusoidal oscillation is assumed to be normally observed. Oscillation amplitude growth and spray angle are maximum compared to the other regimes. Zone C is dominated by the water momentum, and the oscillation growth is limited. This behavior is explained by a competing presence of sinusoidal and dilational waves. Frequency f_{osc} is also plotted as a function of air velocity u_g. In these plots an approximate linear dependence is expected. It has been shown [1] that this dependence is due to viscous effects. If a straigh line is fitted, the slope can be used to define a non-diensional group, the Strouhal number, if a length scale is also introduced. Commonly, the sheet thickness d_l is used for this purpose, so that the number is defined as St = $\frac{f_{osc} \cdot d_l}{u_g}$. It can be noted that in general, the straight lines adjusted to the measurements in these plots cross the abscissa axis at non-zero values. These velocities are denoted as u_g^* and could represent a minimum velocity value required to sustain a sheet oscillation [1]. Frequency as a function of air and water velocities is also presented in a non-dimensional form, using the already defined St number but taking into account the minimum u_g^*, velocity St^* = $\frac{f_{osc} \cdot d}{u_g - u_g^*}$ and the Momentum Flux Ratio (MFR) defined as MFR = $\frac{\rho_g \cdot u_g^2}{\rho_l \cdot u_l^2}$.

Sheet thickness d_l=0.5 mm and air channel width d_g=3.45 mm

For this geometry some problems were experienced when assembling the nozzle head, which resulted in a slightly defective flow near the sheet borders. This may be the reason why the frequency measurements are somewhat irregular. However, most of the characteristics of the sheet oscillation can still be observed.

It is interesting to note the abrupt jump for the transition from region B to C in the four lower series of air velocities, and the strong frequency maxima for u_g = 45, 55 and 65 m/s. The transition from region A to B for u_l takes place near 1 m/s.

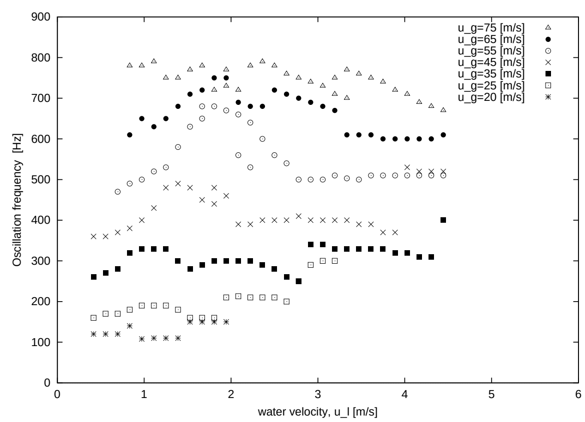

Figure 1: Oscillation frequency f_{osc} as a function of the water velocity, u_l, for the seven air velocities, u_g, with channel exit widths $d_l = 0.5$ mm and $d_g = 3.45$ mm

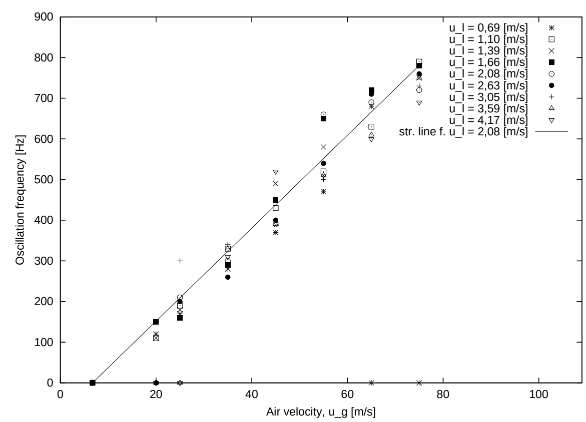

Figure 2: f_{osc} as a function of u_g for nine constant u_l Straight line for $u_l = 1.66$ m/s and $u_g^* = 9.88$ m/s; for $d_l = 0.5$ mm and $d_g = 3.45$ mm

Figure 2 shows the nearly linear dependence on oscillation frequency on the air velocity. For u_l = 1.66 m/s the straight line is plotted. The adjusted line crosses the air velocity axis at u_g^* = 9.88 m/s.

In figure 3 the curves have been collapsed by the introduction of St^* and MFR. In zone B the curves take maximum values near 0.006.

Sheet thickness d_l=0.5 mm and air channel width d_g=10 mm

As can be seen in figure 4 frequency measurements in this conditions are smoother than those in the preceding one, but their values are quite similar even though the air channels are 3 times wider.

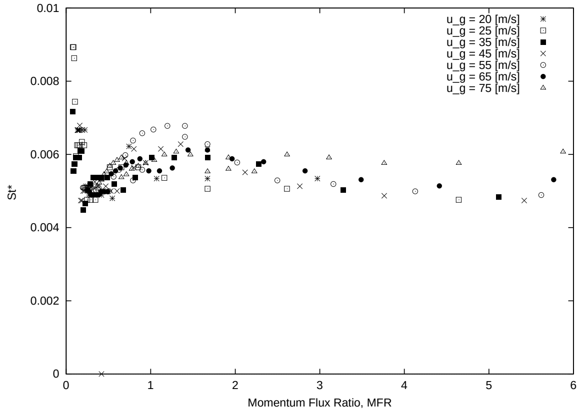

Figure 3: St^* as a function of MFR for the seven u_g, with $d_l = 0.5$ mm and $d_g = 3.45$ mm

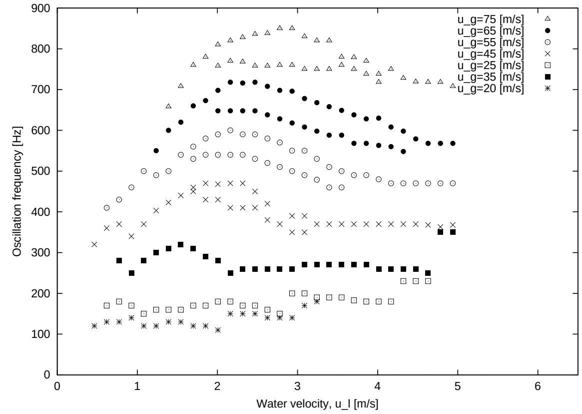

Figure 4: f_{osc}, as a function of u_l for seven u_g; with $d_l = 0.5$ mm and $d_g = 10$ mm

An interesting, and somehow unexpected feature, is a bifurcation that has been measured for air velocities over $u_g \geq 45$ m/s. The water velocities for which the bifurcation starts range between 1.66 < u_l < 2.1 m/s and it closes between u_l = 3.2 m/s and u_l = 4.4 m/s. For these regions, the FFT-power spectrum presents two main peaks with comparable height. For u_g = 35 m/s the curve is similar to the lower branch of the bifurcated ones.

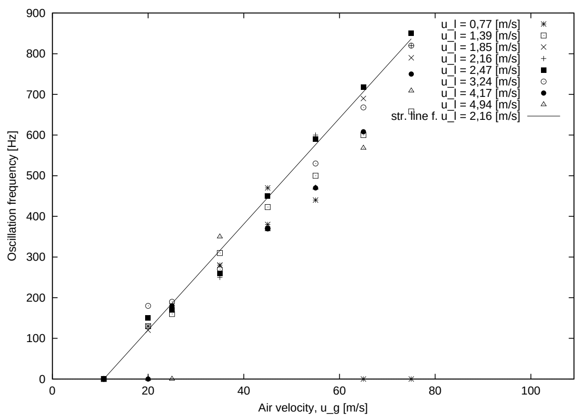

Figure 5: $f_{osc} = f(u_g)$ for seven u_l, $u_g^* = 10.68$ m/s; $d_l = 0,5$ mm and $d_g = 10$ mm

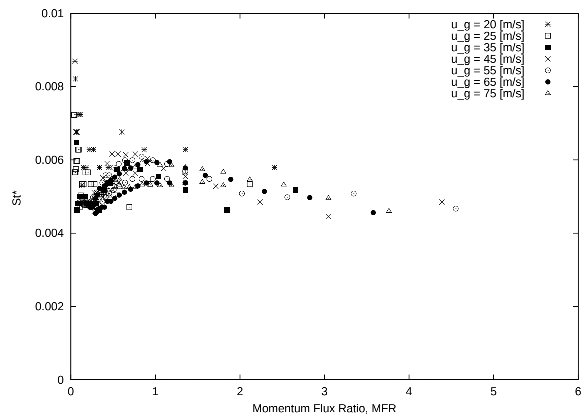

Figure 6: St^* in function of MFR for the seven u_g, with $d_l = 0.5$ mm and $d_g = 10$ mm

In figure 5 approximate linearity is again evidenced. The fitted straight line corresponds to u_l = 1.85 m/s, its slope is 12.68 and u_g^* = 10.68 m/s.

Sheet thickness d_l=0.5 mm and air channel width d_g=35 mm

Only six air velocities have been studied with this air channel thickness because the flow rate produced by the fan was not high enough to reach 75 m/s at the exit. The most remarkable feature of the measurements in this geometry is that the oscillation frequency values are substantially lower than in the preceding cases, as depicted in figure 7. For the highest air velocity u_g = 65 m/s, the maximum frequency has been measured to be f_{osc} = 500 Hz, which is 200 Hz lower than the corresponding value for d_g = 10 mm (figure 4), at the same u_l. A f_{osc} = 500 Hz was obtained with the other air channel widths d_g (figures 1 and 4) for an air velocity of 55 m/s. The curves for u_g in figure 7 are similar in shape to the lower branch of the bifurcated lines in figure 4. The decrease in oscillation frequency gets reflected in its plot as a function of air velocity (figure fig:boq05c35nuralin). The linear dependence yields now a slope of 8.93 for u_l = 2.08 m/s, lower than in the previous geometries.

As figure 9 shows, the values of St^* as a function of MFR, are also quite low, situated around 0.005 without a clear decrease when passing from zone B to zone A. The higher St^* is achieved for the lower air velocity, u_g = 20 m/s, and values decrease as the air velocity increases, especially in zone B.

The first conclusion of these measurements is the obvious dependence of the oscillation frequency on the air channel width. A St^* number defined without inclusion of a parameter somehow indicative of the air channel

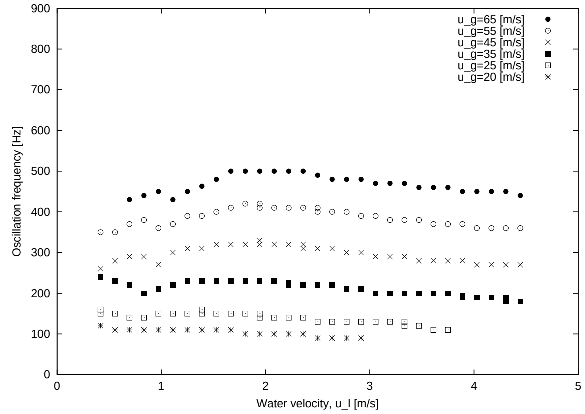

Figure 7: f_{osc} as a function of u_l for six u_g; $d_l = 0,5$ mm and $d_g = 35$ mm

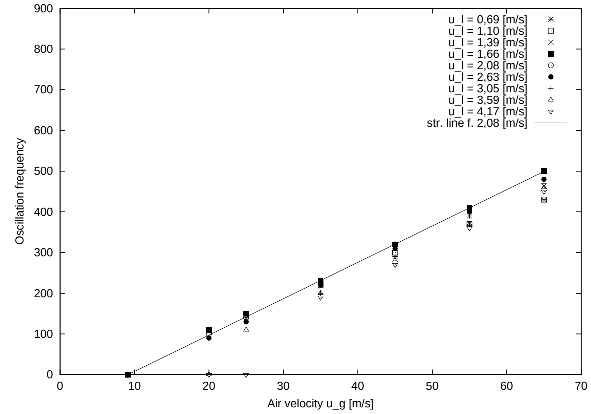

Figure 8: f_{osc} as a function of u_g for nine u_l; $u_g^* = 9.11$ m/s, d_l=0.5 mm and d_g=35 mm

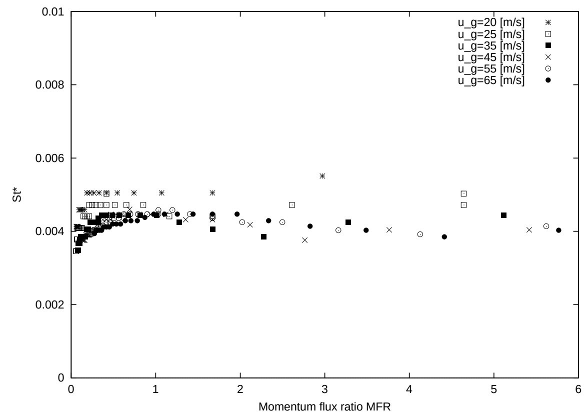

Figure 9: St^* as a function of MFR for the six series of u_g; $d_l = 0.5$ mm and d_g=35 mm

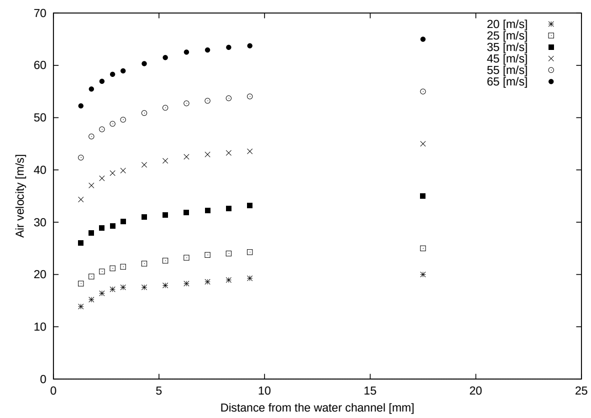

Figure 10: Profiles of u_g in the air channel of $d_g = 35$ [mm] in function of the distance from the water channel.

width will be unable to completely characterize the process. The decrease of St^* with air velocity suggests the dependence not on channel width itself, but of air boundary layer thickness. It is obvious that the reduced contraction ratio results in a wider boundary layer thickness. Finally, comparing the results obtained with the different geometries, it is also evident that the dependence is much weaker than linear.

These results are in agreement with those obtained in [1] using a linear instability study including the viscous effects for both the water and air flows. This numerical analysis demonstrated the importance of the air boundary layer thickness in the frequency established in the liquid sheet. It was observed that increasing the thickness causes a decrease in the wave growth rate, as well as in the wave number for which the maximum growth is reached. This is also accompanied by a reduction in the oscillation frequency. A thicker air boundary layer acts to damp the oscillation of the liquid sheet, simultaneously reducing the maximum growth rate and the frequency for which this maximum is attained, and increasing the wavelength of the propagating perturbation. The different results for the oscillation frequency depicted in figures 4 and 7 yields the necessity to know the air velocity profile just at the exit of the nozzle, where the interaction between air and water is more intense, determining the liquid sheet behavior [7]. For this reason the velocity distribution on the exit section of the air channel was measured for d_l = 35 mm using a calibrated Pitot tube, as shown in figure 10 for the different values of air velocities u_g. Measurements were taken from a distance as close as possible from the water channel wall to a farthest position located 9.3 mm away from the nozzle exit section. The nearest position to the stainless steel piece was with the Pitot pipe just touching the water channel. As the external diameter of the Pitot pipes was 2.6 mm, the first velocity measurement point was taken at 1.3 mm. As can be seen, the air velocity profiles strongly decrease towards the water channel, determining the air boundary layer thickness. Some measurements performed for the thinner air channel (d_g = 3.45 mm) and estimations according to the boundary layer theory [5], [6] indicate a boundary layer thickness thinner than 0.8 mm for u_g = 25 m/s. This scenario could reasonably explain the reduction in the oscillation frequency results obtained for the wider air channel. Again, more experimental measurements are needed to obtain a dependence law to explain the frequency variation.

Sheet thickness d_l=0.9 mm and air channel width d_g=3.45 mm
Figure 11 shows the frequency results corresponding to this configuration, plotted as a function of water velocity for the different air speeds. It is to be noted that as the controlled parameter was the water flow rate, maximum water exit velocities are lower than in the previous cases. Results are in good agreement with those of figures 1 and 4. For all the air exit velocities, the curves have a maximum oscillation frequency in zone B. Transitions to zone A and zone C can be inferred in both extremes of the curves. For d_l = 0.9 mm, frequencies f_{osc} are clearly lower than those corresponding to thinner sheets with the same air channels. Comparing figs. 11 and 1 it might be concluded that oscillation frequency varies with the inverse of the square root of the liquid sheet thickness. Some further experiments would be required to confirm this possibility.

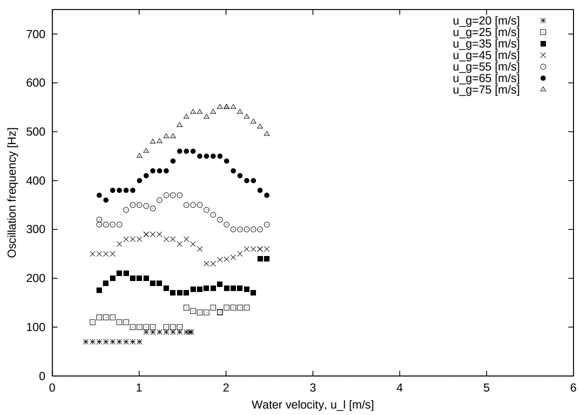

Figure 11: f_{osc}, in function of u_l for the seven u_g; with d_l=0,9 mm and d_g=3.45 mm

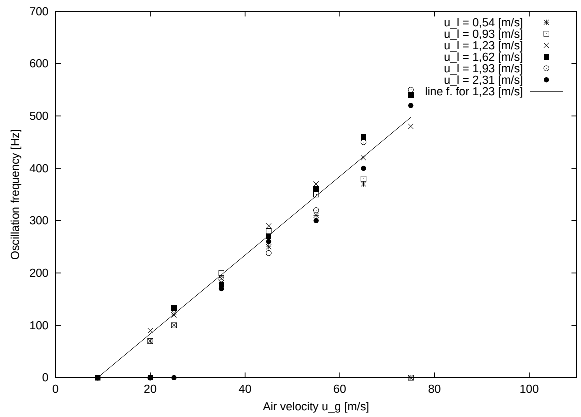

Figure 12: $f_{osc} = f(u_g)$ vs. u_l, $u_g^* = 8.877$ m/s, d_l=0.9 mm, d_l=3.45 mm

The plot of figure 13 is shifted to higher MFR due to the lower values of u_g. The maxima of f_{osc} are found at $MFR \approx 2$.

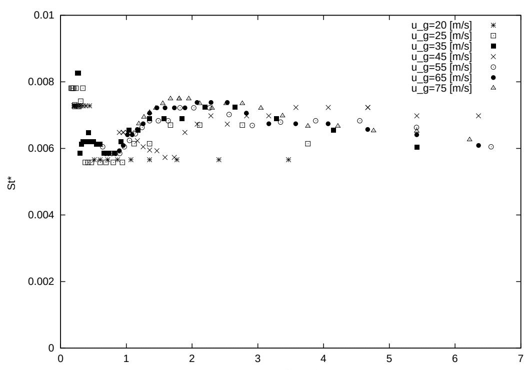

Figure 13: St^* as s function of MFR, for the seven series of u_g, d_l=0.9 mm and d_g=3.45 mm

Conclusions
A study has been performed to study the influence of air co-flow geometry on the oscillation of a liquid sheet. The oscillation frequency has been measured for several air channel widths and different sheet thickness. When varying the channel width from 3.45 mm to 10 mm, maintaining the same conditions for the liquid sheet, the oscillation frequency does not seem to be altered. As a minor difference it might be pointed out that the oscillation frequency maxima for fixed air velocities and varying water velocities, as well as the St^* appear to occur for lower values of the MFR, although in both geometries close to MFR = 1. For d_g = 10 mm a bifurcation in the frequency

versus water velocity curves is observed when the air velocity u_g is higher than 35 m/s, suggesting a competition between two different oscillation modes. It could be due to a superposition of a Kelvin-Helmholtz instability mechanism initiated from the parallel air and water streams, together with a Karman type air vortex detachment at the nozzle lip. When the air channel width is increased to 35 mm, the situation changes visibly. The sheet oscillation frequency is substantially reduced compared to the previous cases. The reduction is more noticeable, roughly by a 1.5 factor for the higher air velocities. These effects appear to be indicative of a dependence of the oscillation frequency on the air boundary layer thickness. The bifurcation disappears, and the frequency curves resemble in shape the lower branch of the bifurcated cases. The 1.5 factor could be related to a square root of the boundary layer thickness.
In this case, the St^* values are obviously lower, but is it also clear that this non-dimensional group has to be redefined if it is intended to reflect all the physics of the problem. Values of the MFR for which the oscillation frequency and St^* are also close to 1.

For the liquid sheet thickness of d_l= 0.9 mm, an oscillation frequency reduction is also observed. This frequency variation, however, does not seem to scale linearly with the thickness. The present measurements might suggest a square root dependence, but further experiments are required to confirm this hypothesis. It is also noticed that in this geometry, the maximum frequencies are achieved for higher values of MFR, closer to 2 instead of 1 as with the thinner sheet.

For all the experiments, a nearly linear dependence of oscillation frequency on air velocity for fixed water speed has been observed. It can also be remarked that in all cases, the fitted straight lines do not cross the abscissa axis (air velocity) in the origin, but on a non-zero positive value. This value could be assigned to a minimum air velocity (or maybe air-water velocity difference) required for the sheet to oscillate. This linearity justifies the use of the non-dimensional Strouhal number, St^*, to characterize the problem, but, as has already been pointed out, the influence of sheet thickness and air boundary layer has to be correctly considered. Further experiments are required to complete this study. Experiments are in course, analyzing more intermediate air channel widths.

Acknowledgements
The first author gratefully acknowledges the regional government of Aragón (Spain) for supporting his activities with a fellowship grant. This research has been supported in part by the project BFM2000-1328 of the Spanish Ministry of Science and Technology

References

[1] Lozano, A., Barreras, F., Hauke, G., Dopazo, C., Longitudinal Instabilities in an Air-Blasted Liquid Sheet, *J. Fluid Mech.*, vol 437, 143 173, 2001

[2] Arai, T., Hashimoto, H., Disintegration of a thin liquid sheet in a concurrent gas stream, *3rd Intl. Conference on Liquid Atomization and Spray Systems, ICLASS-85*, London, U.K, 1985

[3] Mansour, A. and Chigier, N., Dynamic Behavior of Liquid Sheets *Phys. of Fluids A*, vol. 3, (12), 2971-2980, 1991

[4] Hardalupas, Y., Primary Breakup of Coaxial Airblast Atomisers *14th. Annual Conference on Liquid Atomization and Spray Systems*, ILASS-Europe 1998, Manchester, U.K., 1998

[5] Schlichting, H., Boundary Layer Theory, *McGraw Hill*, 6. edition, 1950, London.

[6] Spurk, J.H., Strömungslehre, *Springer*, 3. edition, 1993, Berlin.

[7] Lozano, A., Barreras, F., Experimental Study of the Gas Flow in an Air-blasted Liquid Sheet, *Experiments in Fluid* 31: 367-376 (2001)